European Geothermal Congress 2013
Pisa, Italy, 3-7 June 2013

Enhanced Geothermal System in the Lower Carboniferous in the Netherlands – a geological risk and modelling study

Richard Rijkers[1], Kees van der Hoorn[1], Klaas van Gijtenbeek[2], Robert te Gussinklo Ohmann[3], Gerrit Nitters[1], Bernd Rombout[1], Chris Spiers[4] & Bas de Zwart[1]

[1] IF Technology, Velperweg 37, 6800 AP Arnhem, The Netherlands

[2] Halliburton Columbusstraat 19, 7825 VP Emmen, The Netherlands

[3] Holland Drilling Group, Hooglandpad 6, 8302 KR, Emmeloord, The Netherlands

[4] University Utrecht, Budapestlaan 4, 3584 CD, Utrecht, The Netherlands

r.rijkers@iftechnology.nl

Keywords: Lower Carboniferous, heat demand, Enhanced Geothermal System, hydraulic stimulation, geological risks, geothermal modelling, business case, SPOT

ABSTRACT

The objective of this study is to design a deep geothermal heat exchanger for the Parenco paper mill and to quantify the risk in geothermal flow. The study area is geologically located at the northern flank of the Maasbommel High where the top of the Early Carboniferous (Dinantien) limestone reservoir is recognized at a depth of 4300 m.

Two scenarios have been investigated: (1) natural permeability system from karst/geological faults and (2) EGS subsurface heat exchanger with shear or propped fractures. HP-HT laboratory tests were performed with analogue rock samples from the Ardennes area to evaluate the geomechanical and geohydrological behavior and to model the hydraulic behavior of the fractures. A temperature of 170 ºC is calculated from the regional geothermal heat flow in combination with a model of heat conductivities of all overlying formations. Laboratory testing, geological mapping and geo-thermal modeling are carried out to design a geothermal system in the Early Carboniferous limestone. Shear fracturing was eventually not taken into consideration due to expected low differential earth stresses. Hydraulic fracturing was modeled with FracPro PT & MFrac and flow and heat transport through the resulting fracture geometries was modeled with reservoir simulator TOUGH2.

The geothermal scenario to extract heat from natural permeability in karst zones and geological faults has a relative high risk profile that is caused by the poor quality of the available seismic data and the absence of wells to the target formation. However, the geological concept is proven in the Californië geothermal project near the eponymous village in the South of the Netherlands, in the same reservoir (Fig. 1).

The geological risk of the propped EGS is low but system is significantly more expensive due to high costs of high quality proppant and hydraulic gel that are recommended because of the expected high in situ earth stress (35 MPa), temperature (T> 180 °C) and rock strength (σ_c=50 MPa). Further investigations and 3D seismic data are needed to lower the risk profile of the geothermal project.

1. INTRODUCTION

The initial objective of this study is to design a geothermal system for Parenco paper mill in the Netherlands and to quantify the risk in geothermal flow. The risks involved are largely due to geological uncertainties a lack or quality of seismic data. The geothermal heat shall be used by the Parenco paper mill in Renkum and can also feed the local heat demand in the region at the southwestern area of Arnhem (Fig. 1). A geothermal flow rate of 120 kg/s and minimum input temperature of 160 ºC was taken initially to make an economic business case for the geothermal heat in the low pressure steam system. The geothermal energy is explored in the direct surroundings of the paper mill (<10 km) to prevent high transportation costs.

2. GEOLOGICAL MODEL

2.1 Structural framework

Subsurface structure and tectonic history are regionally well known and described by Duin et al. (2006). The targeted reservoir is the Carboniferous Limestone. This limestone has been deposited in a lower ramp/reef geological facies that is recognized in cores, logs and seismic data on paleo-highs as the London Brabant Massif, Peel Block and Groningen Platforn. The regional distribution of carbonate platforms in northwestern Europe has been recently reported by Van Hulten (2012). This map is shown in figure 1. Lower carboniferous limestones are present and have significant thickness near the structural highs during the Early Carboniferous.

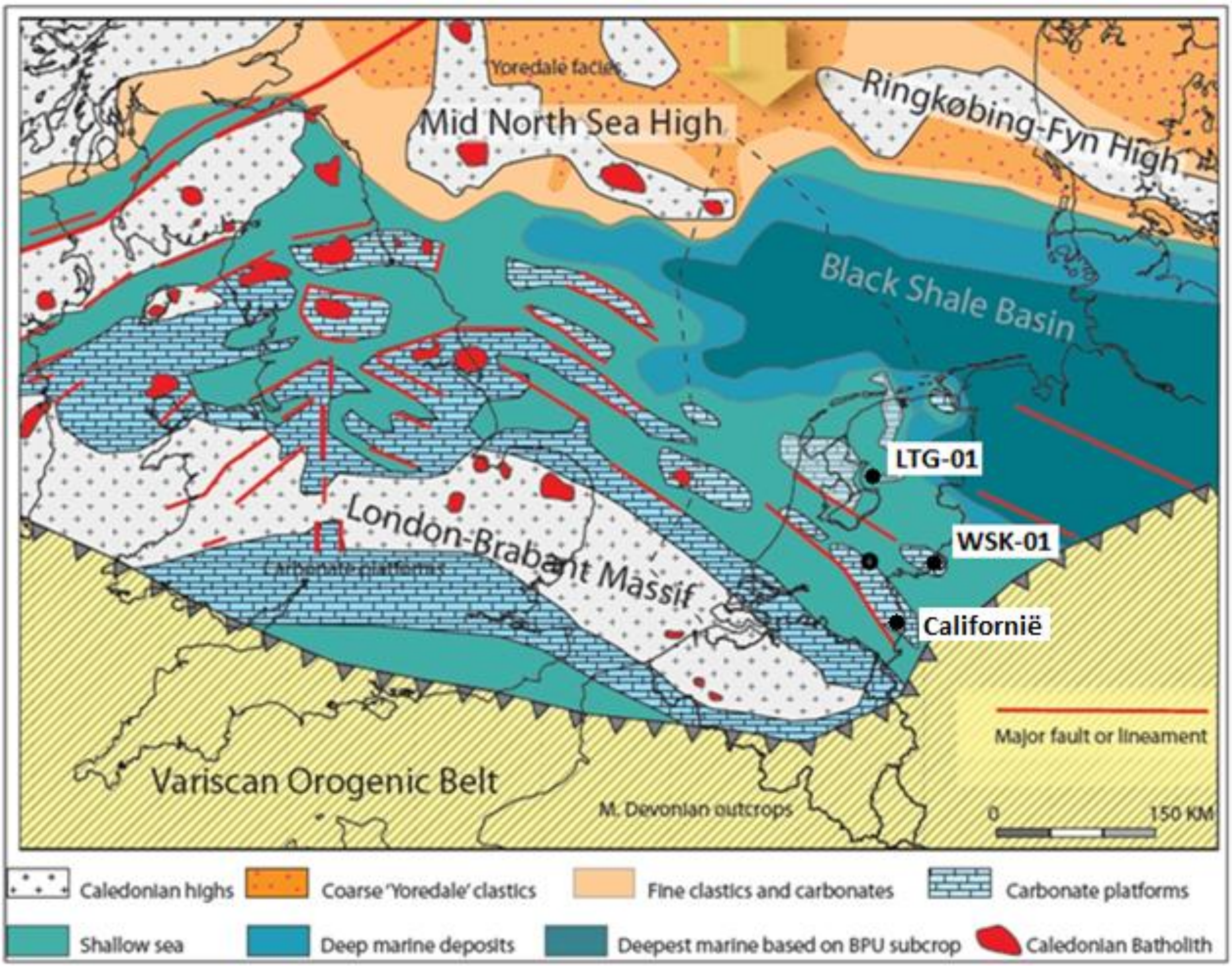

Figure 1 Carboniferous framework and project location.

In available 2D seismic data the top of the Carboniferous Limestone strata is recognizable as a characteristic series of high amplitude reflections. According to the seismic study and comparisons with seismic sections from Kombrink (2010) in Friesland, it is concluded that Parenco is situated at the edge of the Maasbommel High at a depth of approximately 4,300 m. Because of tectonic uplift in the Central Netherlands Basin Lower and Upper Cretaceous sediments are uplifted and eroded at the project site Parenco. Late Cretaceous tectonic inversion led here to the erosion of Cretaceous sediments in basin areas, while these sediments at the pre-existing highs, such as the Maasbommel High, were left untouched on structural highs (Duin et al., 2006). The occurrence of inversion is supported by the presence of transpressional flower structures and reverse faults that are interpreted from seismic data.

2.2 Early Carboniferous limestone

A general platform-basin facies model has been constructed based on a chronostratigraphic analysis from wells north of the London Brabant Massif (Fig. 2). Several periods of sea level low stands have been interpreted based on karst (solution limestone) levels in Visean limestones of the Zeeland Formation. The limestone itself has generally very low matrix permeability, but the karst levels have locally sufficient permeability and connectivity to constitute a good geothermal reservoir. Recently, these Dinantien limestones have been drilled successfully in a nearbygeothermal project, approximately 70 km to the south (Fig. 1).

2.3 Fault and karst potential

Several geothermal projects have been developed in karstified and/or fractured limestones. Most famous projects are located in Lardarello, Italy and Unterhaching, Germany, but also the project in Venlo produces from a combination of karst and fractures in limestone drilled for geothermal purposes near the city of Venlo at a depth of 1,800m.

The main fault direction in the area of interest is NW-SE. This orientation is consistent with the main structures in the Netherlands. A second set of faults has been interpreted and has a NNE-SSW orientation. A regional stress analysis based on literature and breakout analysis of well Luttelgeest-01 indicates that the minimal horizontal stress has a NW-SE direction. In combination with the current extensive regime in the Netherlands, active faults with a NW-SE orientation have higher chances for geothermal water due to high fault dilatancy.

An indicative fault map based on the 2D seismic data has been constructed and is presented in figure 3 along

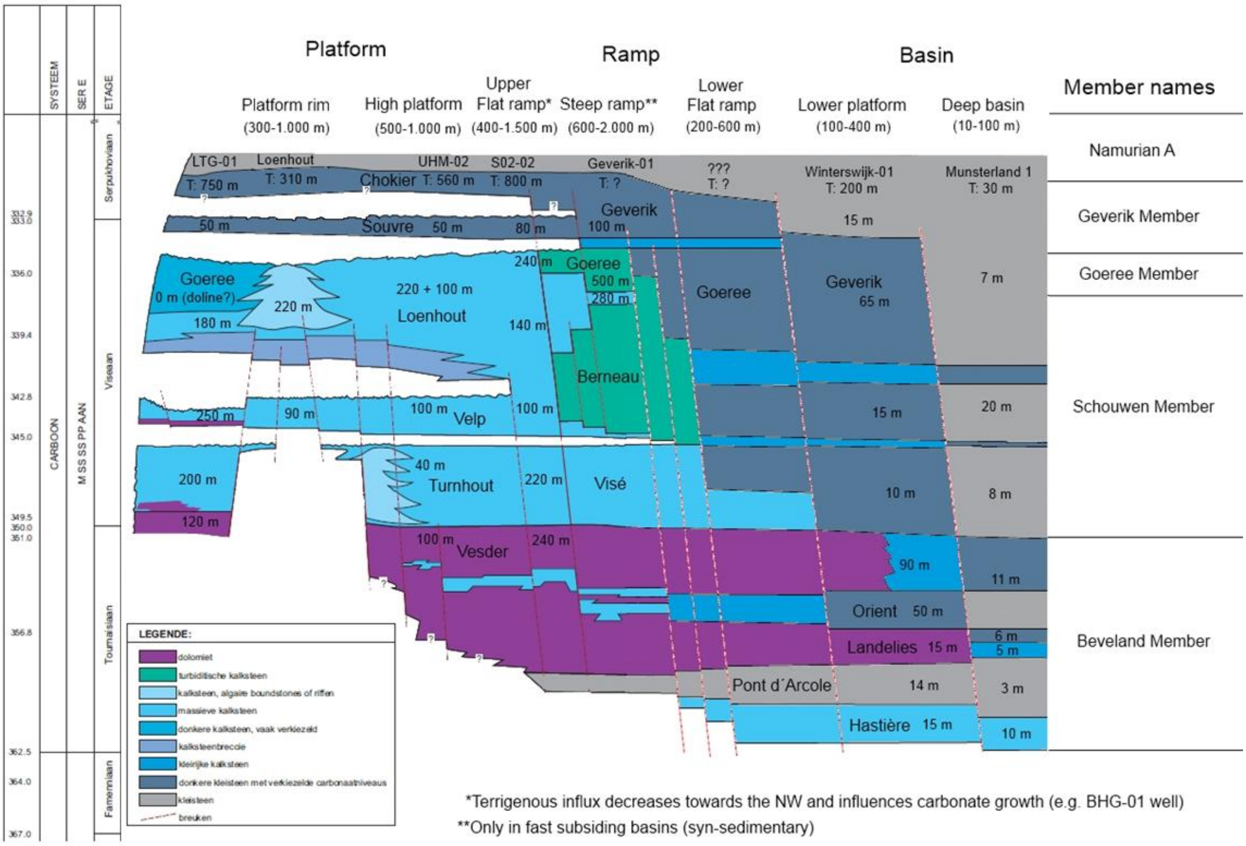

Figure 2 Geological facies model for Dinantien and karst features in the top section.

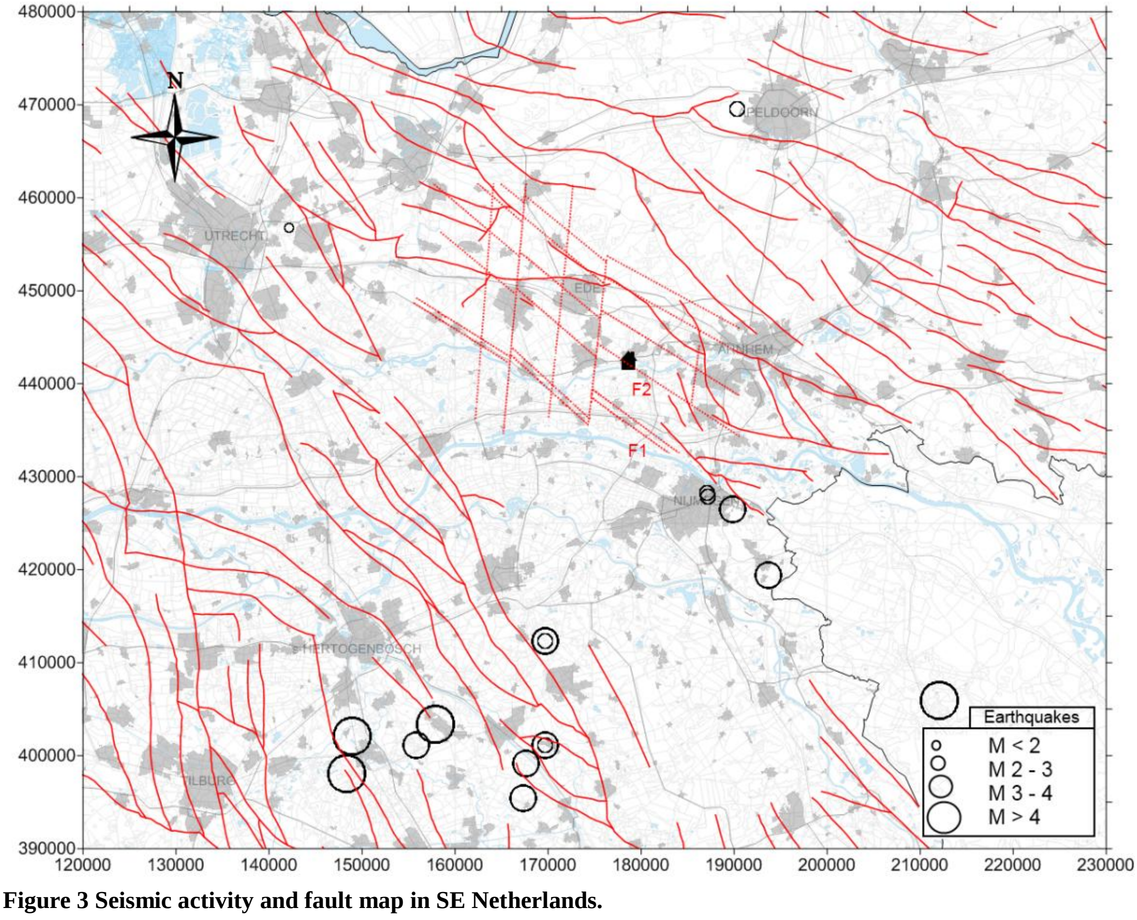

Figure 3 Seismic activity and fault map in SE Netherlands.

with earthquakes and a regional fault map at Zechstein level. The earthquakes near Nijmegen align well with F1 in figure 3. A seismic analysis suggests that F1 has a vertical throw of about 400 m. The orientation of the fault, the extent of the throw and the recent seismic activity make this fault a potential geothermal reservoir. F1 is situated about 6 km southwest of the Parenco site. Fault F2, which is situated below the project location, is estimated to have significantly less potential than fault F1. Fault F1 is characterized by a high vertical throw (>400m) which has been reactivated during Tertiary times.

The conductivity of F1 might not be sufficient to acquire the desired flow of 120 kg/s. Additional flow can possibly be obtained from karst levels. The current seismic data is not of sufficient quality to determine the presence of karst, so at the moment the presence of karst can only be estimated based on analogous examples.

The chances for and extent of karst generally increases towards the rim of carbonate platforms. This is due to a lower water table and an increase in sink holes and sinking streams towards the edge of carbonate platforms. The presence and extent of the karst network can possibly be confirmed by acquiring new high quality seismic data with Amplitude Versus Offset (AVO).

3. ROCK PROPERTIES

3.1 Geomechanical parameters

Available log and core data from Dutch wells Luttelgeest-1 and Winterswijk-1 (location, see figure 1) indicate the matrix permeability of the target limestone is very low, in the order of tenths of microdarcies. At the HPT laboratory at Utrecht University, triaxial and permeametry measurements were performed to investigate the mechanical and transport properties of the intact and fractured limestone. The goal of the measurements was to acquire data on the geomechanical properties of the limestone and to investigate the permeability increase after shear fracturing.

Core samples from the Dutch wells were not available. Therefore, limestone samples from the same geological formation were taken from two Belgian quarries. The calcite content in these samples is similar to that of the Dutch limestone (~99%). The grain sizes from the two quarries were coarse and fine respectively. Firstly, argon transient step permeametry measurements have been performed on the intact limestone samples. The permeability is in the order of 20 nD (20 e-21 m²), for both the fine- and the coarse-grained samples. This is considerably lower than values from the Dutch wells, which are in the order of 0.01 to 1 mD. It is assumed that this discrepancy is of minor influence on the tri-axial tests.

Tri-axial compression tests were performed on rock cylinders measuring 25 mm in diameter by ~57-60 mm length. Tests were performed at temperatures of 150ºC at confining pressures of 30 and 65 MPa, using an axial strain rate of ~10^{-5} s^{-1}. Due to the low permeability of the intact samples, establishing a pore pressure equilibrium corresponding to the in-situ pore pressure (~45 MPa) was not possible. Instead, the compression tests were performed 'dry' at a ~0 MPa pore pressure. All tests showed quasi-elastic, near-linear loading followed by yield. Corresponding Young's moduli (E) measured are 30-48 GPa, depending on the type of sample and confining pressure. All samples deformed in the semi-brittle regime, nearing the brittle-ductile transition at a confining pressure of 65 MPa (Fig. 4).

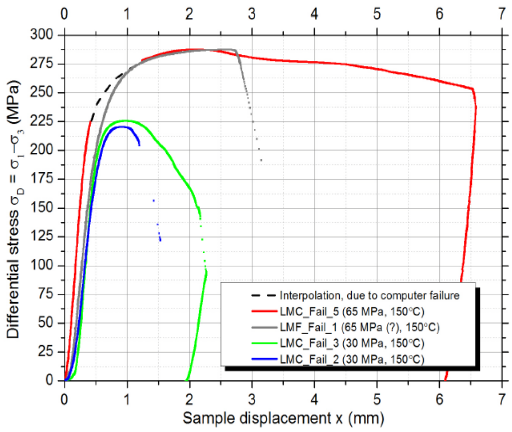

Figure 4 Geomechanical tests results (stress-strain curve).

After shearing of the sample, the permeability of the samples was re-determined to yield a fault zone permeability. This was performed at in-situ pressure conditions and room temperature. Permeability measurements on the fractured cylinder were performed using either the carbonate sand collars or fine drill holes to access to fault. The difference between these results is minor. These results are then translated to apparent fault zone permeability. The results are listed in table 1.

Table 1 Pre- and post-fracturing permeability.

Eff Pc (MPa)	Intact perm (mD)	Fractured perm (mD)	Perm increase
30	$0.24*10^{-4}$	0.27	10,000
65	$0.24*10^{-4}$	$0.73*10^{-2}$	~300

The resulting shear fracture permeabilities are still under 1 mD. It has to be noted that fractures created by fluid injection will likely have a higher permeability. The high compressional forces during the lab tests have created fault zone that is filled with gouge and small fragments. A shear fracture induced by fluid injection will likely have a higher porosity. Shear fractures created by fluid injection are therefore expected to have higher permeability.

3.2 Shear fracturing

Figure 5 shows the local stress situation and the failure envelope obtained from the tri-axial compression tests,

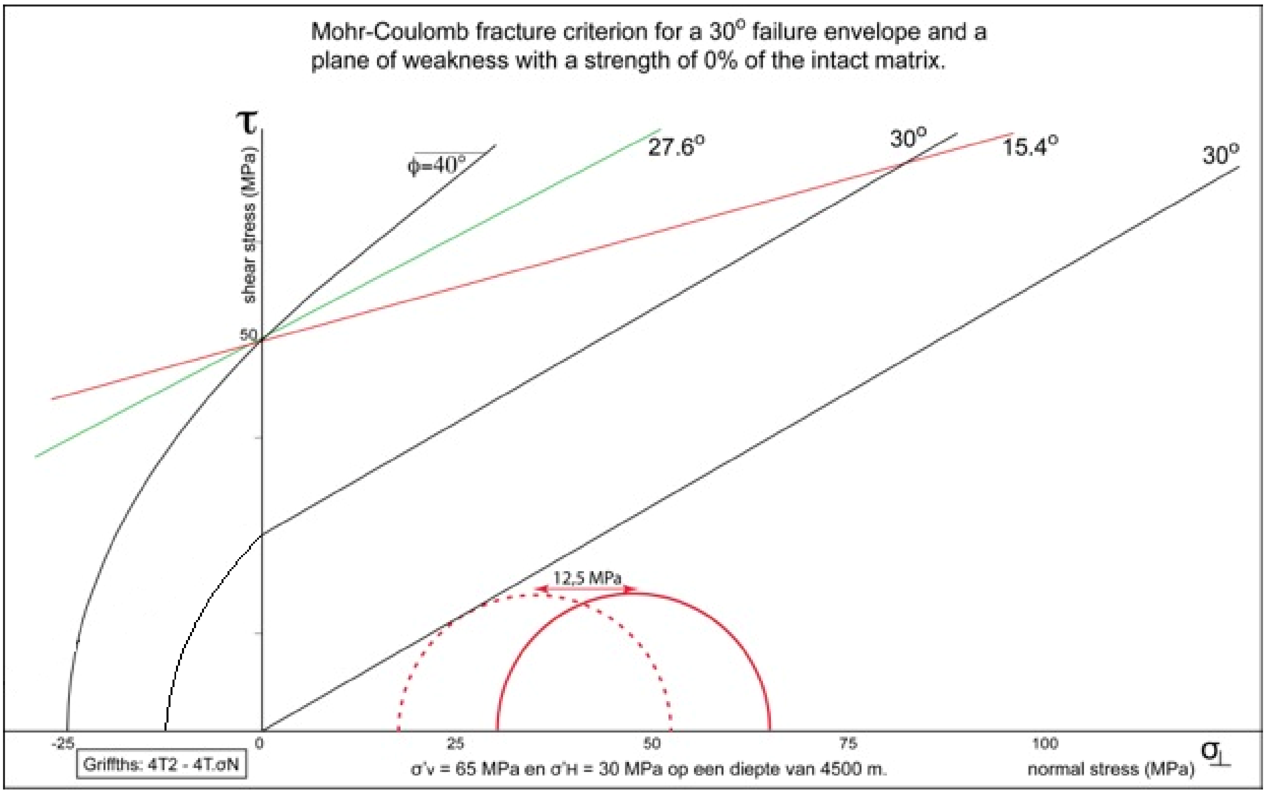

Figure 5 Mohr-Coulomb diagram with envelopes based on test results and local stress at project location.

on the intact samples. The cohesion of the intact limestone is 50 MPa. The other two, outer right failure envelopes are estimates for a pre-fractured rock with a cohesion of 25 MPa and a pre-fractured rock with no cohesion. The latter is an extreme situation, but the Mohr circle shows this is the only situation in which shear failure will occur as the pore pressure is increased.

The differential stress below the project location is low. Therefore, shear failure will not occur through fluid injection in intact rock. Only if the cohesion is very low there is a chance of shear failure, but due to the low differential stress the displacement is expected to be minor. The potential of hydraulic shear fracturing through fluid injection is therefore considered to be low.

4. GEOTHERMAL MODEL OF SUBSURFACE HEAT EXCHANGER

4.1 Propped fracture model

Conventional geothermal production from the target limestone is not possible due to its low matrix permeability. Information on pre-existing natural fractures that might be conduits for fluid flow is very limited. Therefore, as an alternative to the fault/karst scenario, creating a subsurface heat exchanger through a fractured system is presented. Previous studies indicate this artificial reservoir should look like figure 6. Fractures are being created from the middle - production - well. The fracture tips are penetrated by two injection wells to establish circulation of fluid. If the matrix permeability is indeed extremely low, this can be a closed system. The target limestone is a suitable rock for the application of hydraulic fracturing because of its brittleness. Poisson's ratio is ~0.3, Young's modulus is between 30-65 GPa. Its low permeability implies a very high fluid efficiency during a fracturing treatment. One of the most important unknowns is the presence of pre-existing natural fractures which could influence fracture geometry, orientation and treatment design parameters.

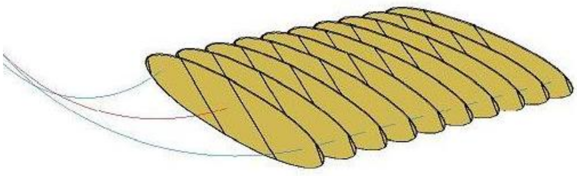

Figure 6 Schematic of the subsurface heat exchanger

In current modelling exercises, the rock matrix permeability was increased slightly to account for some degree of natural fracturing. A linear increasing stress profile was used as a best guess for the minimum horizontal stress below the project location.

In previous studies an ideal fracture design was obtained from fracture and reservoir simulations with MFrac and TOUGH2 (Van der Hoorn et. al, 2012). The ideal design facilitates a high enough flow rate without causing significant thermal breakthrough in the production well within 30 years. For this, a number of approximately 20 fractures is required. The previous fractured design from Van der Hoorn et. Al. (2012) is slightly revised. The goal is to see if the treatment costs per fracture could be reduced by decreasing proppant mass, and to increase proppant quality and fracture conductivity.

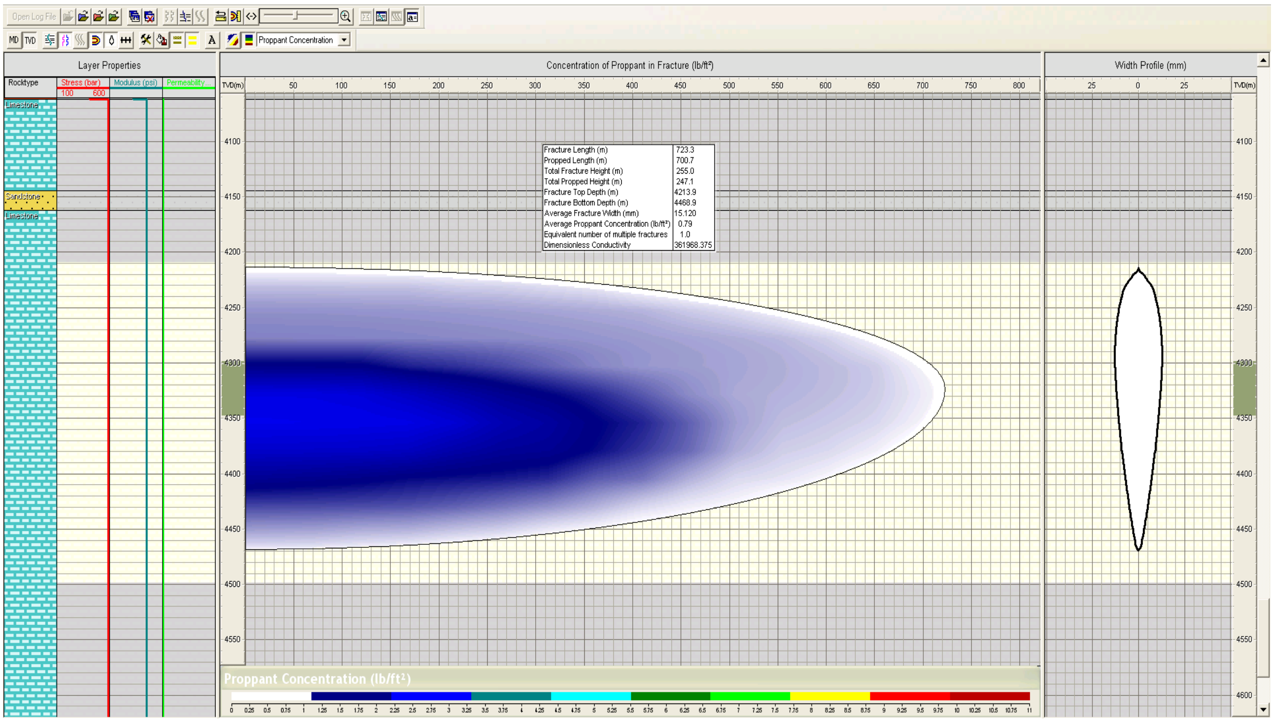

Figure 7 Visualization of ideal fracture design.

The fracture design that was obtained from joined fracture modelling with FracPro modelling software (FracPro, 2012) is shown in Table 2 and figure 7.

The values in table 2 are averages over the particular fracture dimension. This fracture geometry is input for a reservoir model in which hydraulic and thermal effects are calculated. This fracture design is only slightly different from earlier calculations performed with MFrac by IF Technology (Van der Hoorn et. al, 2012). The proppant mass was greatly reduced, but the fluid volume was increased. In the total treatment costs, there is no significant difference. The depth of the target reservoir implies the closure stress on the proppant pack is high. A high quality proppant is required to prevent a decrease in fracture conductivity with time. The effect of pressure dissolution at contacts was not investigated.

Table 2 Ideal fracture design geometry

Frac length (m)	Frac Height (m)	Frac width (mm)	Frac perm (D)	Frac cond (mDm)
700	250	3.7	200	360

4.2 Reservoir model

The revised fracture design is put into a reservoir simulator to mode flow and heat transport. For this the TOUGH2 reservoir simulator and the PetraSim post-processor (Pruess et al, 1999; Thunderhead Engineering) are used. It is assumed that the created fractures will extend symmetrically from the producer to the two injectors. To reduce modelling time, the fracture is also assumed to be symmetrical in height and width so that 1/8 of the total two-winged fracture is modelled. The fracture length determines the well spacing. In addition, it is assumed that the fractures do not interact thermally and therefore can be treated separately. This was checked during previous modelling studies. The reservoir matrix is of very low permeability. The fractures create the necessary permeability for flow to take place between the wells. The fracture is represented in the models as a zone of high permeability grid blocks in the reservoir matrix. These grid blocks extend from the injector to the edge of the producer as shown in figure 8.

To model a uniform horizontal cell size equivalent to the fracture width would be impractical, requiring an extremely large number of cells. Therefore, the method of grid doubling was applied. The cell size in the wells is similar to the expected inner-pipe diameter. In addition, given the technique proposed to create the fractures (proppant injection) a degree of porosity is retained inside the fracture. The permeability and porosity of the fracture are assumed to be uniform along the fracture in the horizontal and vertical (when used) directions. The matrix and fracture characteristics are listed in Table 3.

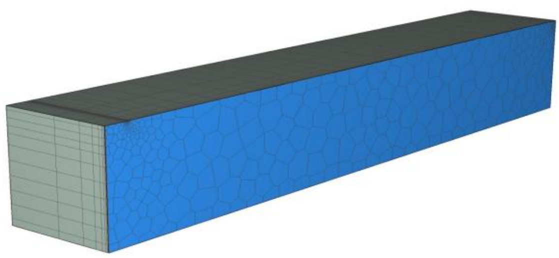

Figure 8 Grid of matrix/fracture reservoir model. (fracture plane in blue)

Table 3 Reservoir properties

	Permeability (mD)	Porosity (%)	Thermal conductivity (W/mK)
Matrix	1	0.01	2.8
Fracture	200,000	0.3	2.3

Previous calculations concluded that approximately 20 fractures are required to facilitate a flow rate of 120 kg/s without causing thermal break trough. This implies a flow rate of 6 kg/s per fracture. This number is divided by 8 due to symmetrical splitting of the model domain. For a period of 30 years, this flow rate is injected continuously with a temperature of ~85ºC. The initial model temperature, and therefore production temperature, is ~165ºC. Figure 9 and 10 shows the temperature evolution in the production well and model domain after 30 years of continuous production. Less than 1ºC temperature cooling is calculated in TOUGH2. Fluid flow takes place primarily through the high conductivity fracture. Heat exchange between fluid in the fracture and the surrounding rock matrix takes place primarily through conduction.

The calculated pressure drop over the reservoir is ~135bar. This pressure drop is added to the pressure loss in the pipes to calculate a total dP over the system and to calculate the Coefficient of Performance, the ratio of the heating provided over the electrical energy consumed for the subsurface geothermal system.

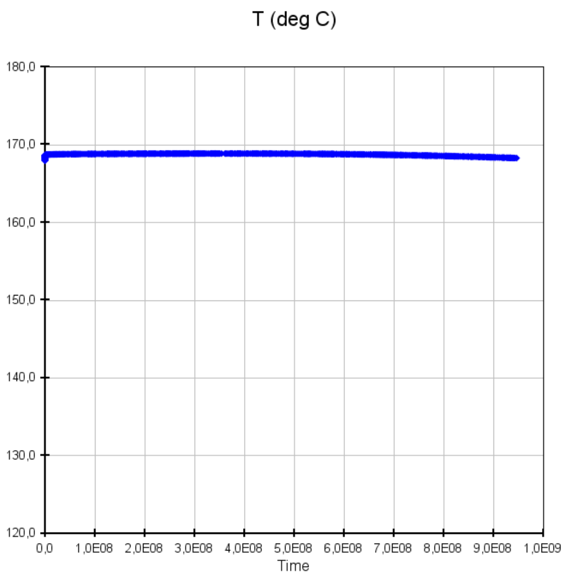

Figure 9 Temperature evolution in production well after 30 years.

5. QUANTITATIVE RISK ANALYSIS

A numerical risk analysis is performed on the previous results to quantify the probability of achieving a flow rate of 120 kg/s. The fracture design model and reservoir model require input from literature, well log and laboratory measurement.

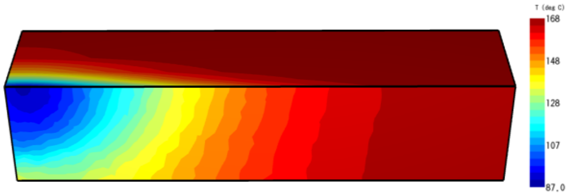

Figure 10 Temperature distribution in model domain after 30 years of injection and production.

These are all prone to some degree of uncertainty and are summarised in Table 4). To capture this uncertainty in the final result, the flow rate, a series of Monte Carlo analyses is performed. The input is varied independently for each input parameter. Each input parameter has its own probability distribution, determined from the log, seismic, core or laboratory measurements. A similar analysis is not possible for the karst/fault scenario because there is a lack of data.

The risk analysis can be subdivided into two modeling stages: 1) the fracture design model and 2) the reservoir model. The results of the fracture design model are input for the reservoir model and calculate the geothermal flow rate through a single fracture. The 3D fracture design and reservoir software that were used in previous calculations are not compatible with running a Monte Carlo simulation. Therefore, simplified, analytical models were used to perform this task. Both the analytical fracture geometry calculator adopted from Economides et. al (2002) and a reservoir model based on Darcy's Law, calculated similar results to the 3D results. However, several assumptions have been made. The most important is that the fracture height is limited by the formation thickness but can be adjusted if the formation is thicker than the ideal height of 250-300m. Also, the pressure drop over the reservoir is assumed to be constant, for every different realization of fracture geometry and permeability. The most important input parameters and their probability distribution are given in table 4.

Table 4 Overview of Monte Carlo input

Parameter	**Min**	**Most likely**	**Max**
T at top reservoir (ºC)	143	163	180
Depth top reservoir (m TVD)	3,600	4,000	4,400
Thickness reservoir (m)	200	300	400
Fracture permeability (D)	100	200	300
Reservoir permeability (mD)	0.01	0.1	1
Fracture geometry	Monte Carlo results are input for the reservoir model.		

A probability curve of the flow rate in the production well is obtained for a fixed number of fractures, see figure 11. It is found that for 21 successful fractures, the p90 flow rate in the production well is 120 kg/s. For the same number of fractures, the p50 flow rate is only slightly higher. Or alternatively, the same flow rate of 120 kg/s is obtained with 19 to 20 fractures for the p50. It is concluded that the difference between the p90 and p50 cases is small.

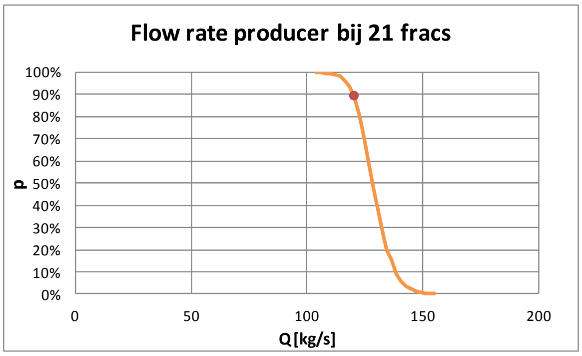

Figure 11 Probability of flow rate for 21 propped fractures.

6. WELL DESIGN

The geothermal doublet consists of two wells heads, one producer and one injector. From the injector well a second injection path will be drilled to the reservoir as a multilateral well. Two scenarios have been modeled. In scenario 1 we assume presence of karst/fractured permeability. In this case the injector main well is drilled sub-vertically to depths of about 2700 meters (TVD). From this point off, a deviation of about 30 degrees is drilled. From the same well a multilateral is drilled in the opposite direction creating two injector wells in the reservoir with a final out step from the producer of 1500 meters on both sides (Fig. 12).

In scenario 2, we assume the EGS multiple propped fracs system to be required for enough flow. In this case two wells are drilled to about 1000 meters above the Dinantien limestone. From this point the wells will be deviated following the slightly dipping reservoir.

In the previous chapter it is indicated that 21 fractures should be created. Assuming a fracture spacing of 150 m (Van der Hoorn, 2012), this implies a horizontal section of about 3000 m will be required for optimal placement of the fractures (Fig. 13). Hydraulic fractures shall be theoretically oriented in the NW-SE direction following the maximum horizontal stress that is derived from regional data and wells.

7. GEOTHERMAL INSTALLATION

The energy concept is based on heat exchanger at surface a twin injector holes to pump the cooled water back in the hot reservoir rock. The subsurface and surface geothermal energy system is schematised in Fig. 14. A production well delivers the heat to a heat exchanger. At temperature of 160°C only low pressure

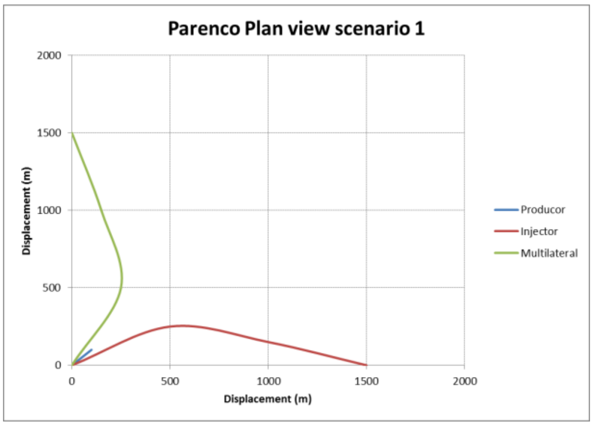

Figure 12 Plan view well path of scenario 1 (natural permeability and karst).

Figure 13 Plan view well path of scenario 2 (propped fractures).

steam and hot water can be produced. The heat exchanger is connected with a distribution net towards the paper mill location at a distance of seven km's. The return temperature in the geothermal water circuit after the steam compression process will be high enough (approx. 93 °C) for use in warm water processes. The geothermal power system is designed to deliver 34 MW for low pressure steam that is used in the production of paper.

8. BUSINESS CASE

The business case was calculated for both scenario 1 (geological faults and karst) and for scenario 2 (propped fracture reservoir). For calculation of the business case of scenario 1, it is assumed that the conductivity of the karst along the faulted zone is high enough to produce 120 kg/s (~ 400 m3/hour). For the calculation of the costs of scenario 2 (propped fractures) it is assumed that the EGS can be engineered following the conceptual design. Eventually, additional hydraulic fractures can be set to increase geothermal heat production.

The karst and natural fractured fault scenario 1 has a IRR of 9.8 %. The geothermal scenario 2 with the propped fractures has an IRR 5.3%. The costs of the proppant and gel for scenario 2 (hydraulic fracturing)

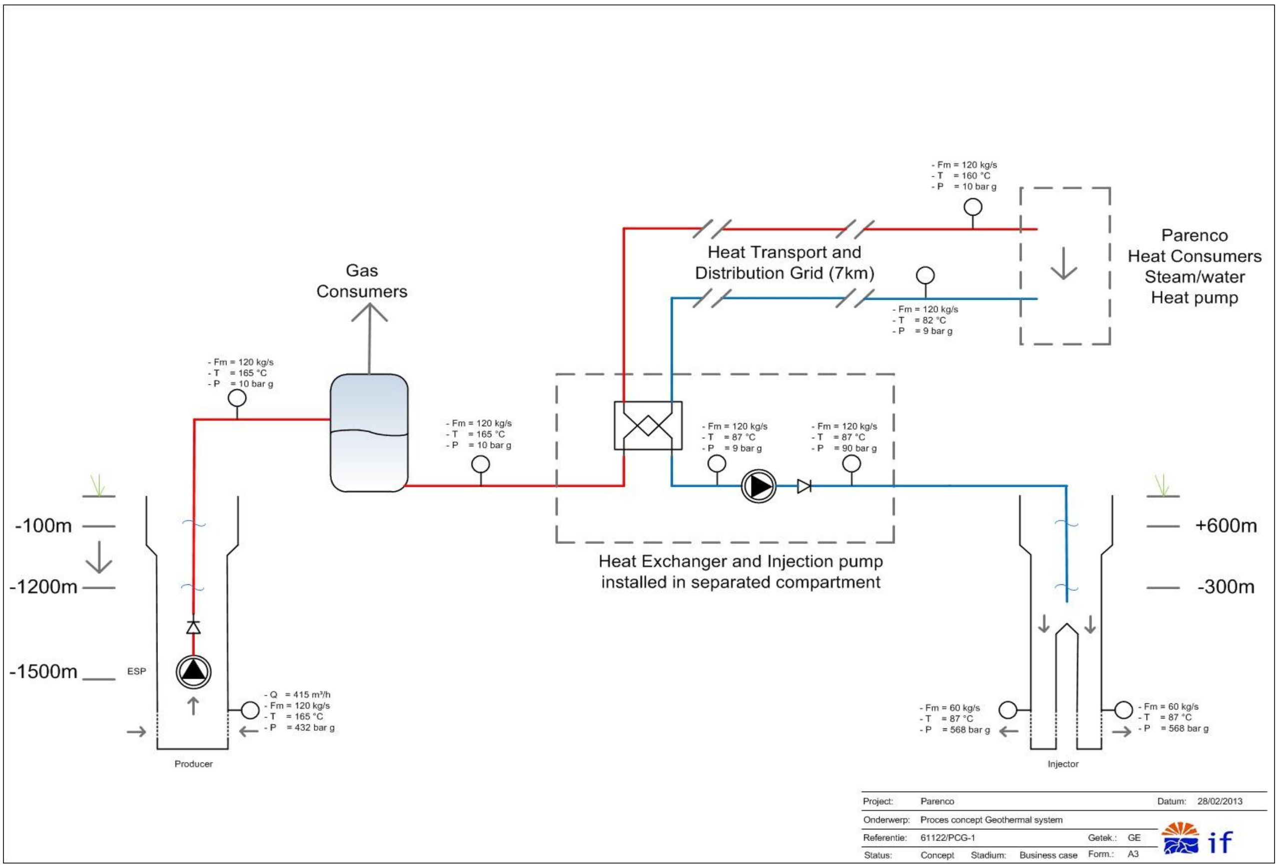

Figure 14 The geothermal installation

are higher in scenario 1 due to the high length of the sub-horizontal well section of 3000 m.

The propped fracture scenario 2 (EGS) is obviously more expensive than scenario 1 where slightly deviated wells are used. When using an artificial high CO_2 prize of 35€/ton in scenario 1 (natural permeability) the SPOT shall only decrease from 7.5 to 6.5 years. In scenario 2 (propped fractures) the SPOT is reduced with the artificial high CO_2 prize of 35€/ton from 14.9 to 12.7 years. Evidently and due to, the higher the CO_2 prize has more effect in the business case of scenario 2:

<u>Scenario 1</u>:	34 MW
Natural	IRR: 9,8 %
permeability	SPOT: 7,5 year (15 €/ton)
	SPOT: 6,5 year (35 €/ton)

<u>Scenario 2:</u>	34 MW
Propped	IRR: 5,3 %
fractures	SPOT: 14,9 year (15 €/ton)
	SPOT: 12,7 year (35 €/ton)

9. CONCLUSIONS

The Lower Carboniferous limestone is most likely present at the northern rim of the Maasbommel High, a geological structure below the Parenco site in Renkum. This is concluded from available 2D seismic data, regional borehole data and structural history and geological facies correlation. The top of the limestone is estimated at a depth of 4,300m and has a temperature of approx. 170°C. The thickness of the formation is estimated at 400m ± 300 depending on the location with respect to the structural high.

The geothermal project location is characterized by Palaeozoic fault systems that have been reactivated during various (recent) tectonic events. This is shown by seismic data and earthquake monitoring towards the southeast. Fault movement in limestone usually leads to enhancement of the natural permeability. The production of geothermal water from a karst/fault zone near the Parenco site is considered to be realistic. It is however difficult to quantify the uncertainty in flow rate with the available data set.

Triaxial and permeametry measurements are taken in a HPT laboratory with in-situ conditions. These indicate that the potential of shear fracturing in the limestone is low. Shear fractures are only likely to form in pre-fractured rock with sufficient differential earth stress.

To quantify the uncertainty in flow rate coming from the subsurface heat exchanger, a Monte Carlo risk analysis is carried out. Geological uncertainties as temperature, depth, fracture geometry and matrix and fracture permeability are input for the model. This resulted in a P90 flow rate of 120 kg/s and a P50 flow rate of 130 kg/s from 21 fractures.

The EGS subsurface heat exchanger is designed and 21 propped fractures are needed to produce 34MW. The costs of the fracturing treatment are high due to the use of special high strength proppant and gel.

The CO_2 prize effect the SPOT in both scenario's. When using a artificial high CO_2 prize of 35€/ton in scenario 1 (natural permeability) the SPOT shall only decrease from 7,5 to 6,5 years.

In order to obtain more reliability of karst zones it is advised to obtain high resolution AVO 3D seismic data. New seismic data is also of great value to map geological faults at depth and to analyse rock property of the Carboniferous Limestone with geophysical methods. Improved fault maps are of great value to reduce risk of seismicity, possibly caused by geothermal drilling and/or production of geothermal water and re-injection of water.

REFERENCES

Duin, E.J.T, Doornenbal, J.C., Rijkers, R.H.B., Verbeek, J.W., & Wong, Th.E.: Subsurface structure of the Netherlands – results of recent onshore and offshore mapping, *Netherlands Journal of Geosciences,* **85-4**, (2006), 245-276

Economides, M., Oligney, R., Valko, P. (2002). "Unified fracture design". Orsa Press, Alvin, Texas.

Kombrink, H. (2010) The Carboniferous of the Netherlands and surrounding areas; a basin analysis. Geologica Ultraiectina, Volume: 294

Pruess, K., C. Oldenburg, and G. Moridis (1999). TOUGH2 User's Guide, Version 2.0.Report LBNL-43134, Lawrence Berkeley National Laboratory, Berkeley, Calif.

Thunderhead Engineering, PetraSim5 User Manual.

Van Adrichem Boogaert, H.A. & Kouwe, W.F.P. (Eds): Stratigraphic nomenclator of the Netherlands, revision and update by RGD and NOGEPA, *Mededelingen Rijks Geologische Dienst,* **50**, (1993-1997)

Van der Hoorn, K., Heijnen, L.J., Gankema, M.E., Nitters, G. (2012). Hydraulic fracturing in limestone: A case study of two EGS projects in the Netherlands. Proceedings of the Thirty-Seventh Workshop on Geothermal Reservoir Engineering Stanford University, Stanford, California, January 30 - February 1, 2012 SGP-TR-194.

Van Hulten, F.F.N. (2012) Devono-carboniferous carbonate platform systems of the Netherlands. Geologica Belgica 15/4, p. 284-296.

Acknowledgements

We acknowledge the province of Gelderland for financing this study and Joris Spaan of Parenco for authorization to publish the results of this study.